Childs Nerv Syst (2013) 29:1079–1088
DOI 10.1007/s00381-013-2103-y

REVIEW PAPER

# The benefits of navigated intraoperative ultrasonography during resection of fourth ventricular tumors in children

**Mohamed A. El Beltagy · Mostafa M. E. Atteya**

Received: 18 August 2012 / Accepted: 4 April 2013 / Published online: 23 April 2013


**Abstract**
*Background* Safe and radical excision of pediatric fourth ventricular tumors is by far the best line of management. Pediatric fourth ventricular tumor surgery is a challenge for neurosurgeons. The aim of the study is to present the authors' experience and to evaluate the possible benefits of neuro-navigated intraoperative ultrasonography (NIOUS) during the surgery of fourth ventricular tumors in children.
*Methods* Nonrandomized clinical trial study was conducted on 60 children with fourth ventricular tumors who were treated at Children's Cancer Hospital-Egypt. Mean age was 5.2 (±2.6)years. Thirty cases were operated upon utilizing the conventional microneurosurgical techniques. Another 30 cases were operated upon utilizing the NIOUS technique.
*Results* Total tumor excision was achieved in 29 cases (96.7 %) of NIOUS group versus 24 cases (80 %) in the conventional group. Mean operative time NIOUS group was 150 min [standard deviation (SD)=18.28) versus 140.6 min (SD=18.6) in the conventional group ($p$ value=0.055). The mean operative blood loss was 67.5 ml (SD=17) in NIOUS group versus 71 ml (SD=15.4) in the conventional group. Postoperative cerebellar mutism occurred in one case (3.3 %) of NIOUS group versus in six cases (20 %) of the conventional group.
*Conclusions* Integration of navigated intraoperative ultrasonography in surgery of pediatric fourth ventricular tumors is a useful technology. It safely monitors maximum stepwise tumor excision. It is associated with less operative morbidity without significantly added operative time. It is a real-time, cost-effective, easily applicable, and easily interpretable tool that could substitute the use of intraoperative MRI especially in pediatric neurosurgery.

**Keywords** Brain shift · Fourth ventricular tumors · IGSonic · Intraoperative ultrasonography · Image guidance · Neuro-navigation

M. A. El Beltagy (✉) · M. M. E. Atteya
Neurosurgery Department, Children's Cancer Hospital Egypt (CCHE, 57357), Cairo, Egypt
e-mail: beltagy_mohamed@hotmail.com

M. M. E. Atteya
e-mail: dr.mostafa.atteya@gmail.com

M. A. El Beltagy · M. M. E. Atteya
Neurosurgery Department, Kasr Al-Ainy School of Medicine, Cairo University, Cairo, Egypt

## Introduction

Fourth ventricular tumors occur in children more frequently than in adults. Approximately 50–55 % of brain tumors in children are infratentorial [27].

The clinical manifestations of pediatric tumors of posterior cranial fossa usually appear late when the tumor size gets large. Radical surgical removal of these tumors is fairly risky because of the deep location and the close relation to the surrounding brain stem, important nerves, and blood vessels. The most important prognostic factors are the effective rate of surgical removal and avoiding occurrence of severe complications. That's why successful treatment of pediatric fourth ventricular tumors is very challenging for neurosurgeons [4].

Intraoperative ultrasonography (IOUS) was attempted in the 1960s. Now, IOUS is well established as an intraoperative imaging technique in different neurosurgical procedures [1, 6, 7, 9, 10, 14, 15, 18–26].

IOUS is widely used in neurosurgery today. IOUS is very valuable in neurosurgery. It helps in determining tumor location and reducing operative time and hence, provides better surgical efficiency and safety [23].

Following the introduction of navigation technology in the market, the idea of integrating ultrasonography with neuro-navigation systems was proposed [11]. The main limitation of ordinary neuro-navigation systems is the intraoperative brain distortion and shifts that may occur during surgery, the so-called brain shift. However, the brain shift correction could be

made in many neuro-navigation systems after integration of other real-time technologies such as intraoperative magnetic resonance imaging (MRI), computed tomography (CT), or ultrasound [1, 3, 13, 16].

## Methods and materials

### Patient population

This nonrandomized clinical trial study was conducted on 60 children with fourth ventricular tumors who were treated at Children's Cancer Hospital Egypt between January 2008 and October 2012.

Thirty patients were operated upon by conventional micro-neurosurgical techniques without neuro-navigational or intra-operative imaging technologies. This group will be termed the "conventional group." The other 30 cases were treated using microneurosurgical excision with the assistance of neuro-navigated IOUS, and will be termed the "NIOUS group." All study cases were operated upon through telovelar approach in the prone position.

Operative time, operative blood loss, and extent of tumor resection were recorded in all cases. Early postoperative MRI images were obtained for all cases during the first postoperative 48 h. Tumor residue less than 1 cm was considered as "near total resection," while tumor residue more than 1 cm was considered as "subtotal resection."

Clinical assessment during the postoperative period was focusing on the development of cerebellar mutism syndrome. The onset, severity, progression, and duration of the syndrome were assessed. Time to recovery and pattern of recovery were also assessed. The affected component(s) were also recorded whether linguistic, motor, neuro-behavioral, or combinations of all. Mild syndrome was considered if one component only is affected. If two components were affected, this was considered moderate syndrome. And severe syndrome was considered if all components were affected.

### Statistical analysis

Computer software package SPSS 15 was used in the statistical analysis. Categorical data were presented as frequencies and percentage, while continuous data were presented as mean± standard deviation. Pearson Chi-square–Fisher's exact tests were used for the comparisons of proportions. Comparisons between groups were made using one-way ANOVA test. A $p$ value less than 0.05 was considered to be significant.

### Preoperative MRI acquisition and planning

Preoperative MRI studies of the brain and whole spine without and with intravenous contrast were performed for all patients. One or more image sets compatible with BrainLab neuro-navigation system were obtained.

If cerebrospinal fluid (CSF) diversion is to be performed before tumor excision surgery, we operate on recent preoperative MRI BrainLab protocol scans after CSF diversion procedure in order to avoid inaccuracy related to the brain shift that may have occurred due to CSF diversion. Preoperative planning includes outlining the tumor and the brainstem on the BrainLab work station in different colors. This is important in the calculation and correction of brain shift that may occur during the ongoing tumor excision and to reach maximum safe tumor resection during surgery. Following MRI data acquisition and presurgical planning, the processed patient data are then transferred to the intraoperative neuro-navigation system.

### Image guidance system

We made use of BrainLab-Kolibri™ system, a frameless, armless, image-guided neuro-navigation system, based on

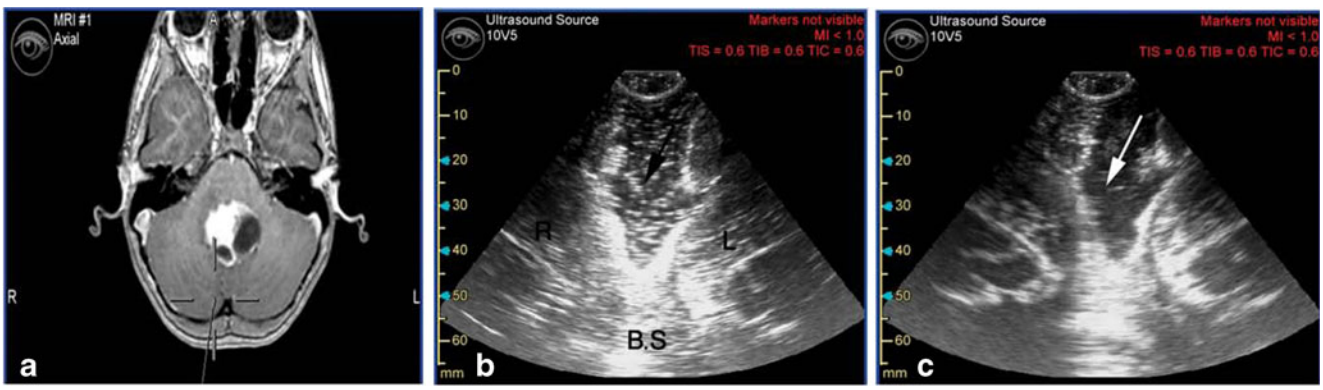


**Fig. 1** A 9-year-old female patient with fourth ventricular pilocytic astrocytoma. **a** Preoperative axial MRI image on screen. **b** Surgical bed during saline wash after tumor excision. Note the characteristic acoustic signal of the turbulent saline that delineates the surgical cavity (*black arrow*). **c** Surgical bed after stoppage of saline wash (*white arrow*). *R* right cerebellar hemisphere, *L* left cerebellar hemisphere, *B.S.* brainstem

passive reflection of infrared light (BrainLab, Heimstetten, Germany). Software update was installed for ultrasound device detection and brain shift calculation and correction.

## Image-guided ultrasonography

The ultrasound device used was IGSonic® 3000 device with a frequency range of 4–9 MHz and a depth of 120 mm at 5 MHz. The probe used was phased array treason 10 V5 with footprint dimensions of 25×15 mm. The 10-V5 probe is calibrated by using ultrasound registration phantom and is integrated into the BrainLab-Kolibri navigation system.

## Technique and image acquisition

The patient is positioned in prone position. The patient's head is fixed to the operating table by Mayfield head holder, and the Mayfield reference array is then attached to it. Image-patient registration fusion is then performed. Image guidance is used to localize the tumor and to study its extensions and relations to major posterior fossa landmarks.

After elevation of the suboccipital craniotomy flap and removal of the posterior arch of atlas, an initial transdural ultrasound examination of the posterior fossa is carried out, focusing on the site, depth, margins, echogenicity, and relations of the tumor, and also on

**Table 1** Clinical data of the cases operated with the guidance of neuro-navigated IOUS (The NIOUS group)

| Case | Age (years) | Sex | Pathology | Excision | Operative time (min) | Blood loss (ml) | Cerebellar mutism | | | | |
|---|---|---|---|---|---|---|---|---|---|---|---|
| | | | | | | | Incidence | Onset (postop) | Duration | Severity | Extent of recovery |
| 1 | 4 | F | Pilocytic astrocytomas | TR | 130 | 50 | No | – | – | – | – |
| 2 | 3 | M | Fibrillary astrocytomas | TR | 170 | 60 | No | – | – | – | – |
| 3 | 7 | M | Meningioma | TR | 140 | 80 | No | – | – | – | – |
| 4 | 7 | F | Medulloblastoma | TR | 140 | 80 | Yes | 3 days | 21 days | Mild | Complete |
| 5 | 2 | M | Pilocytic astrocytomas | TR | 160 | 50 | No | – | – | – | – |
| 6 | 8 | F | Pilocytic astrocytomas | TR | 140 | 100 | No | – | – | – | – |
| 7 | 1.5 | M | Anaplastic ependymoma | TR | 130 | 90 | No | – | – | – | – |
| 8 | 7 | F | Medulloblastoma | TR | 170 | 70 | No | – | – | – | – |
| 9 | 5 | M | Dermoid cyst | TR | 150 | 60 | No | – | – | – | – |
| 10 | 7 | M | Pilocytic astrocytomas | NTR | 140 | 80 | No | – | – | – | – |
| 11 | 9 | F | Pilocytic astrocytomas | TR | 170 | 60 | No | – | – | – | – |
| 12 | 6 | M | Medulloblastoma | TR | 120 | 90 | No | – | – | – | – |
| 13 | 2 | M | Fibrillary astrocytomas | TR | 150 | 60 | No | – | – | – | – |
| 14 | 9 | M | Medulloblastoma | TR | 130 | 70 | No | – | – | – | – |
| 15 | 14 | F | Medulloblastoma | TR | 160 | 80 | No | – | – | – | – |
| 16 | 4 | F | Medulloblastoma | TR | 170 | 50 | No | – | – | – | – |
| 17 | 9 | M | Pilocytic astrocytomas | TR | 160 | 70 | No | – | – | – | – |
| 18 | 4 | M | Fibrillary astrocytomas | TR | 120 | 50 | No | – | – | – | – |
| 19 | 5 | M | Anaplastic ependymoma | TR | 140 | 90 | No | – | – | – | – |
| 20 | 6 | M | Anaplastic ependymoma | TR | 140 | 80 | No | – | – | – | – |
| 21 | 3 | M | Pilocytic astrocytomas | TR | 120 | 40 | No | – | – | – | – |
| 22 | 5 | F | Fibrillary astrocytomas | TR | 175 | 50 | No | – | – | – | – |
| 23 | 4 | M | Medulloblastoma | TR | 160 | 70 | No | – | – | – | – |
| 24 | 2 | F | ependymoma | TR | 140 | 40 | No | – | – | – | – |
| 25 | 7 | F | medulloblastoma | TR | 180 | 90 | No | – | – | – | – |
| 26 | 4 | M | ependymoma | TR | 165 | 60 | No | – | – | – | – |
| 27 | 6 | F | Medulloblastoma | TR | 140 | 50 | No | – | – | – | – |
| 28 | 3 | M | Pilocytic astrocytomas | TR | 185 | 45 | No | – | – | – | – |
| 29 | 8 | M | Medulloblastoma | TR | 155 | 75 | No | – | – | – | – |
| 30 | 6 | F | ependymoma | TR | 150 | 85 | No | – | – | – | – |

*F* female, *M* male, *ml* milliliter, *STR* subtotal resection, *TR* total resection)

**Table 2** Clinical data of the cases operated with conventional microneurosurgical techniques (conventional group)

| Case | Age (years) | Sex | Pathology | Excision | Operative time (min) | Blood loss (ml) | Cerebellar mutism | | | | |
|---|---|---|---|---|---|---|---|---|---|---|---|
| | | | | | | | Occurrence | Onset (postop) | Duration | Severity | Extent of recovery |
| 1 | 1.5 | M | Anaplastic ependymoma | TR | 120 | 60 | No | – | – | – | – |
| 2 | 7 | M | Pilocytic astrocytomas | TR | 130 | 60 | No | – | – | – | – |
| 3 | 12 | M | Medulloblastoma | TR | 130 | 90 | No | – | – | – | – |
| 4 | 7 | M | Pilocytic astrocytomas | TR | 170 | 100 | Yes | Day 1 | 3 weeks | Moderate | Complete |
| 5 | 5 | F | Pilocytic astrocytomas | TR | 140 | 90 | Yes | Day 1 | 5 weeks | Moderate | Complete |
| 6 | 6.5 | M | Medulloblastoma | TR | 170 | 80 | No | – | – | – | – |
| 7 | 1 | M | Fibrillary astrocytomas | TR | 120 | 50 | No | – | – | – | – |
| 8 | 5 | M | Anaplastic ependymoma | TR | 150 | 70 | No | – | – | – | – |
| 9 | 10 | M | Medulloblastoma | TR | 140 | 90 | No | – | – | – | – |
| 10 | 5 | M | Immature teratoma | TR | 160 | 70 | No | – | – | – | – |
| 11 | 3 | M | Anaplastic ependymoma | NTR | 150 | 60 | No | – | – | – | – |
| 12 | 2 | F | Pilocytic astrocytomas | TR | 120 | 60 | No | – | – | – | – |
| 13 | 3 | M | Pilocytic astrocytomas | TR | 150 | 50 | No | – | – | – | – |
| 14 | 5 | F | Fibrillary astrocytomas | TR | 140 | 80 | Yes | Day 0 | 5 weeks | Moderate | Complete |
| 15 | 3 | M | Medulloblastoma | NTR | 180 | 50 | No | – | – | – | – |
| 16 | 2 | F | Medulloblastoma | TR | 170 | 60 | No | – | – | – | – |
| 17 | 7 | F | Pilocytic astrocytomas | TR | 150 | 80 | No | – | – | – | – |
| 18 | 4 | M | Medulloblastoma | TR | 120 | 70 | No | – | – | – | – |
| 19 | 6 | M | Pilocytic astrocytomas | TR | 130 | 80 | No | – | – | – | – |
| 20 | 7 | F | Astrocytomas with pilomyxoid features | STR | 150 | 110 | Yes | Day 1 | 6 months | Severe with upper limb monoparesis | Complete |
| 21 | 8 | F | Medulloblastoma | TR | 160 | 80 | Yes | Day 0 | 2 months | Severe | Residual ataxic dysarthria |
| 22 | 5 | M | Ependymoma | TR | 130 | 80 | No | – | – | – | – |
| 23 | 4 | M | Medulloblastoma | TR | 120 | 70 | No | – | – | – | – |
| 24 | 8 | F | Ependymoma | TR | 160 | 65 | No | – | – | – | – |
| 25 | 3 | M | Pilocytic astrocytomas | NTR | 135 | 55 | No | – | – | – | – |
| 26 | 5 | M | Medulloblastoma | TR | 110 | 80 | No | – | – | – | – |
| 27 | 5 | F | Medulloblastoma | NTR | 130 | 60 | Yes | Day 1 | 4 weeks | Moderate | Complete |
| 28 | 2 | M | Fibrillary astrocytomas | TR | 125 | 50 | No | – | – | – | – |
| 29 | 4 | F | Pilocytic astrocytomas | TR | 140 | 60 | No | – | – | – | – |
| 30 | 3 | M | Ependymoma | STR | 120 | 70 | No | – | – | – | – |

*F* female, *M* male, *ml* milliliter, *STR* subtotal resection, *TR* total resection

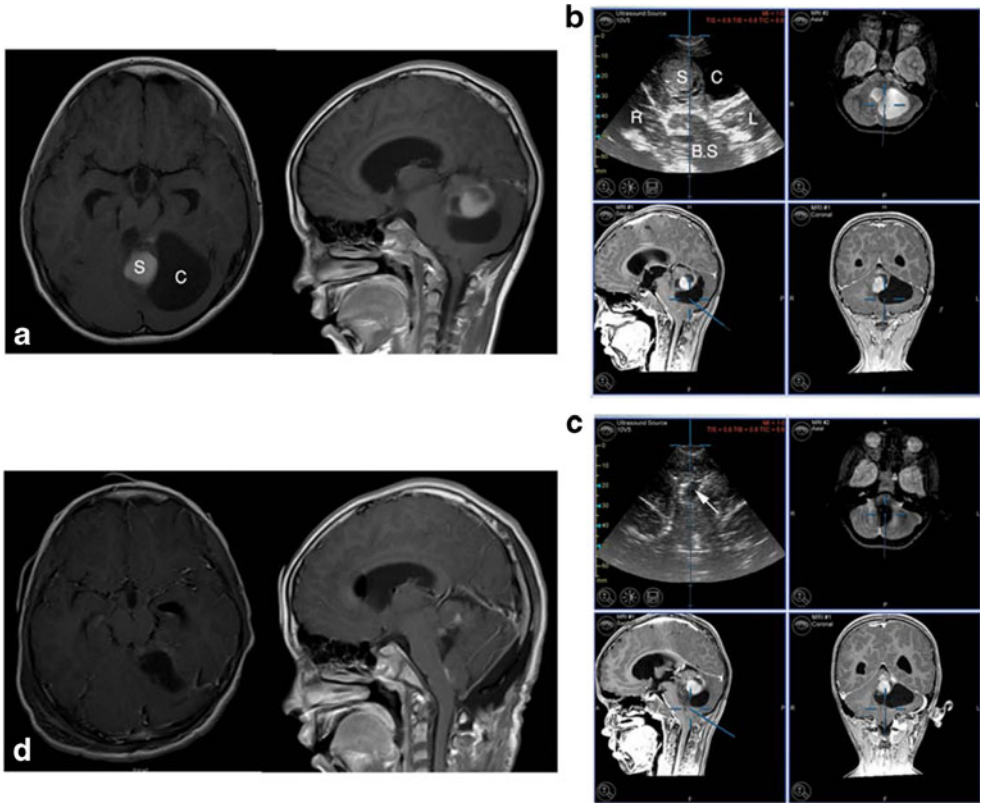


**Fig. 2** A 9-year-old male patient with left cerebellar glioma. **a** Preoperative MRI images, tumor has a solid medial component (*S*), and a cystic lateral component (*C*). **b** NIOUS assessment of the tumor and its relations in posterior fossa. **c** Final assessment after tumor excision, surgical cavity partially collapsed and filled with saline (*white arrow*). **d** Early postoperative MRI shows total tumor excision. *S* Solid medial component, *C* cystic lateral component, *R* right cerebellar hemisphere, *L* left cerebellar hemisphere, *B.S.* brainstem

the surrounding posterior fossa structures including the cisterna magna.

Then, landmarking of the vascular anatomy using power color Doppler mode is carried out focusing on the vascularity of the tumor, relations to major surrounding vessels, and checking the presence of a capacious occipital or marginal dural sinuses which, if torn, may cause troublesome bleeding and air embolism during dural opening.

Then, the cisterna magna is opened to drain CSF followed by cautious Y-shaped dural incision avoiding injury to the dural

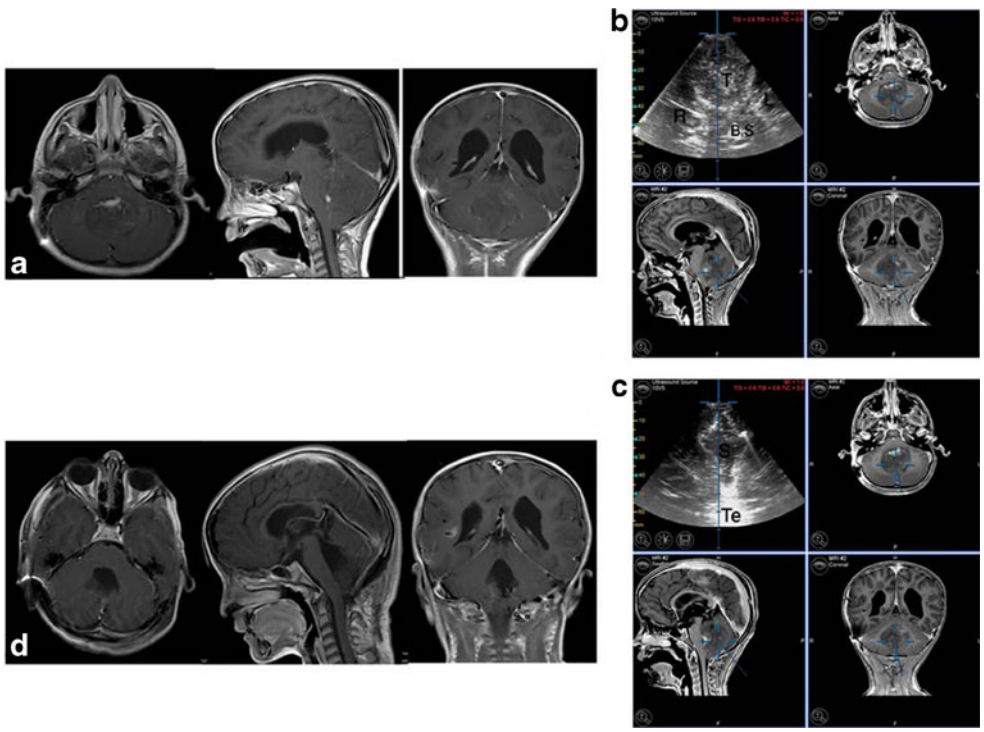


**Fig. 3** A 6-year-old male patient with huge fourth ventricular medulloblastoma. **a** preoperative MRI images. **b** NIOUS examination during ongoing tumor excision shows the tumor (*T*) and its relations. **c** NIOUS examination after tumor excision, surgical bed filled with saline. **d** Early postoperative MRI shows total tumor excision. *T* Tumor, *R* right cerebellar hemisphere, *L* left cerebellar hemisphere, *B.S.* brainstem, *s* saline filling the surgical cavity after tumor excision, *Te* tentorium cerebelli

sinuses. Then, another ultrasound examination is performed with the ultrasound probe being directly placed on the cerebellum, and tumor localization is again verified. Stepwise resection of the tumor is guided by subsequent NIOUS as needed. Imaging is performed in two perpendicular planes.

Posterior fossa anatomical landmarks such as the tentorium cerebelli, brainstem, fourth ventricle, and the cerebral aqueduct should be clearly identified in relation to the tumor during surgical resection. Surgery through the telovelar approach was performed in all cases.

The technique of image fusion for the preoperative MRI data set overlaid with the intraoperative real-time 3-D ultrasound images was used to appreciate and calculate the brain shift that occurs after dural opening, CSF drainage, and ongoing tumor resection.

Image artifacts can occur due to air bubbles, blood clots, or cottonoids in the surgical field. Continuous irrigation of the surgical cavity with saline together with removal of blood clots and air bubbles during performing image scans is important to obtain clear images.

Saline turbulence during irrigation of the surgical field is a useful acoustical marker [5]. It gives characteristic mottled acoustical signals of the surgical cavity that disappears when irrigation is stopped. This "on and off" method of saline irrigation helps to accurately define the surgical bed and its margins as shown in Fig. 1.

It's also important to avoid applying too much coupling contact gel at the tip of the ultrasound probe before it is enclosed in the sterile sheath. Then, probe's sterile sheath and draping of the probe are smoothed out to remove all folds. This will help achieve good quality images.

### Image interpretation

In our initial experience with NIOUS, a neuro-radiologist had to attend operation in order to help us interpret the ultrasound images [5]. By time, we passed through a learning curve and started to use and interpret NIOUS without a neuro-radiologist. Fusing three-dimensional ultrasound images with preoperative MRI images is performed to calculate brain shift.

## Results

### Demographic characteristics

The study included 60 children harboring fourth ventricular tumors (38 males and 22 females). The mean age was 5.2 years (SD=2.64). The NIOUS group was comprised of 18 males and 12 females with a mean age of 5.5 years (SD=2.7). The conventional group was comprised of 20 males and 10 females with a mean age of 4.9 years (SD=2.5). The youngest case in the study was a 1-year-old male with fibrillary astrocytoma, while the oldest case was a 14-year-old female with medulloblastoma. Tables 1 and 2 show the clinical data of the study groups.

### Extent of resection

In the NIOUS group, total excision was achieved in 29 (96.7 %) cases, and near-total excision was achieved in 1 (3.3 %) case. In the conventional group, the excision achieved was a total excision in 24 (80 %) cases, while non-total excision was detected in 6 (20 %) cases [near-total excision in 4 (13.3 %) cases, and subtotal excision in 2 (6.6 %) cases].

Figures 2, 3, 4, and 5 show stepwise resection in different cases of fourth ventricular tumors as compared with early postoperative MRI scans. Small residual tumor was observed at the pre-final ultrasound examination, which was located in the lateral recess of fourth ventricle in two cases, and ventral to the rostral part of inferior cerebellar vermis in two cases.

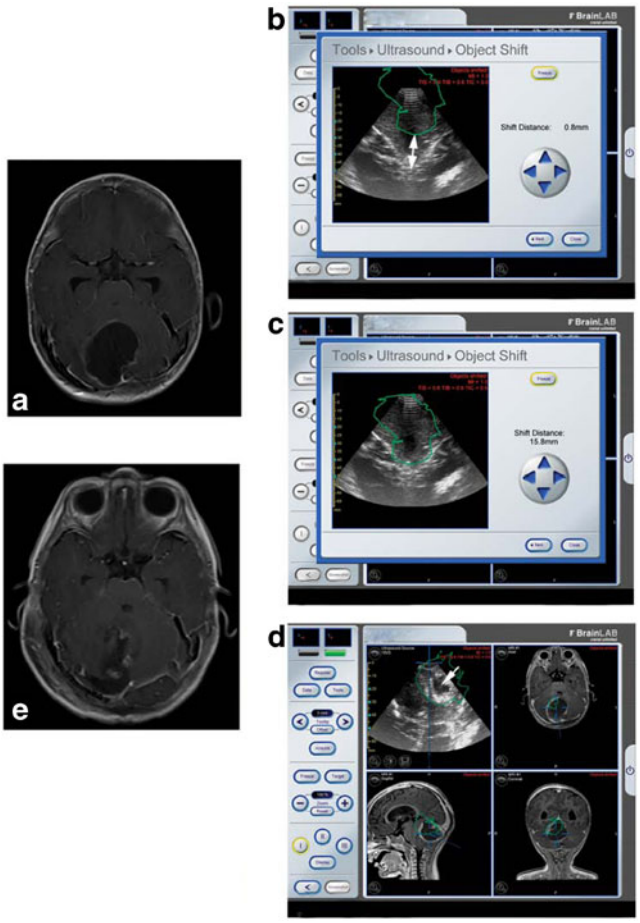


**Fig. 4** A 2-year-old male patient with cystic diffuse fibrillary astrocytoma. **a** Preoperative axial MRI. **b** Measuring the brain shift, shifting distance between the pre-planned tumor (in *green*), and the intraoperative real-time shifting distance (*double head white arrow*).**c** NIOUS examination after a shift of 15.8 mm was appropriately corrected. **d** Surgical bed after tumor excision filled with saline and partially collapsing (*single head arrow*). **e** Early postoperative axial MRI shows total tumor excision

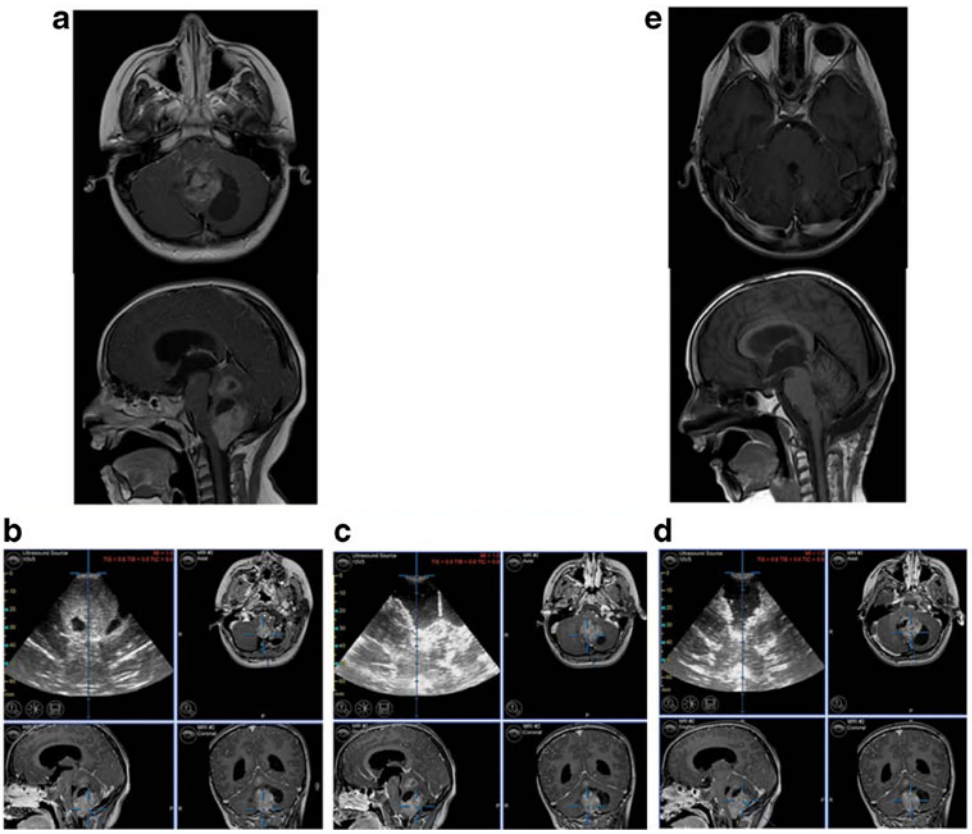


**Fig. 5** A 9-year-old male patient with fourth ventricular medulloblastoma. **a** Preoperative MRI images. **b** Initial NIOUS examination of the posterior fossa. **c** Subsequent examination showing residual tumor. **d** Final NIOUS examination showing total tumor excision and surgical bed filled with saline. **e** Early postoperative MRI shows total tumor excision

Figure 6 shows a case of fourth ventricular astrocytoma with pilomyxoid features with a small tumor residue detected in the early postoperative MRI scans. Table 3 shows the statistical analysis regarding extent of tumor excision.

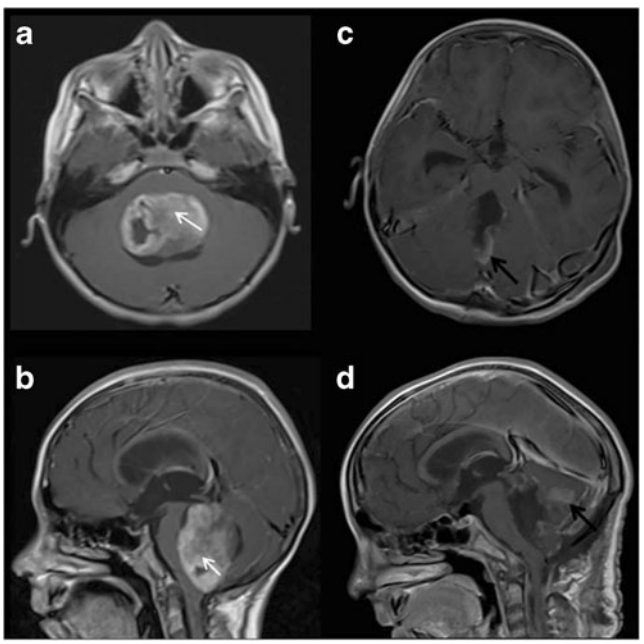


**Fig. 6** A 7-year-old female patient with fourth ventricular astrocytoma with pilomyxoid features. **a**, **b** Preoperative MRI images (*white arrows*). **c**, **d** Early postoperative MRI images showing a small tumor residue (*black arrows*)

### Operative time

The mean operative time in cases guided with NIOUS was 150 min with standard deviation of 18.28 min as compared with 140.6 min with standard deviation of 18.6 min in the conventional group. This difference is not statistically significant ($p$ value=0.055).

### Intraoperative blood loss

The mean intraoperative blood loss in cases guided with NIOUS was 67.5 ml with standard deviation of 17 ml as compared with 71 ml with standard deviation of 15.4 ml in cases operated by conventional neurosurgical techniques. Table 4 shows the statistical analysis of blood loss and operative time.

### Assessment of cerebellar mutism

In the NIOUS group, cerebellar mutism occurred in one case only (3.3 %), while within the conventional group, cerebellar mutism was postoperatively encountered in six cases (20 %). Table 3 shows the statistical analysis of cerebellar mutism.

**Table 3** Distribution of sex, cerebellar mutism and degree of resection differences among the study groups

| Variables | Overall, *n* (%) | Conventional group, *n* (%) | NIOUS group, *n* (%) | $\chi 2$ | *P* value |
|---|---|---|---|---|---|
| Sex | Male 38(63.3) | 20 (66.7) | 18 (60.0) | 0.07 | 0.78 |
| | Female 22 (36.7) | 10 (33.3) | 12 (40.0) | | |
| Cerebellar mutism | Yes 7 (11.7) | 6 (20) | 1 (3.3) | 4.043 | 0.103 |
| | No 53 (88.3) | 24 (80) | 29 (96.7) | | |
| Resection degree | TR 53 (88.3) | 24 (80) | 29 (96.7) | 4.043 | 0.103 |
| | Non-total excision (NTR+STR) 7 (11.7) | 6 (20) | 1 (3.3) | | |

*NTR* near total resection, *n (%)* number and percentage, *STR* subtotal resection, *TR* total resection, $\chi^2$ Chi- square

## Discussion

Although intraoperative MRI and CT scans are useful, they are expensive and are only available in few centers. NIOUS is a reliable real-time technique for assessing tumor size, defining tumor margins, and for detecting residual tumors [5, 8, 12, 17].

The use of NIOUS to update preoperative images has been considered. NIOUS is relatively an inexpensive technology. Also, it allows fast multiplanar imaging and can reliably detect residual tumors [2].

When intraoperative neuro-navigation systems are used without being combined with a real-time intraoperative imaging modality, they provide non-real-time images that may be misleading. This is due to the fact that they are based on image sequences that are obtained preoperatively. Navigation based on old and un-updated preoperative images will neglect the dynamic brain shifts that occur during surgery such as ongoing tumor resection, CSF drainage, and drained tumor cysts.

On the other hand, using ordinary intraoperative ultrasonography without neuro-navigational guidance, despite being real time, could also be confusing. That's because there are many confusing acoustic signals such as difficult identification of normal brain tissue around tumors especially gliomas, peri-tumoral edema, and surgical bed changes.

Coupling of neuro-navigational guidance together with the real-time intraoperative ultrasonography gives real-time imaging and appreciates brain shifts. And if brain–tumor interface is in doubt due to confusing acoustic signals, this could be overcome by double checking of direct visual input from the operating microscope together with the neuro-navigational input.

So, coupling of direct visual input, real-time ultrasound images, and neuro-navigational data augments the benefits and minimizes the drawbacks of utilizing any of them separately. At any time during stepwise tumor resection, we were able to detect tissue shifts, correct shift, update new scans by NIOUS, verify new tumor site by neuro-navigated pointer, and simultaneously confirm all these by direct visual input from the surgical microscope. Fusion of preoperative MRI images together with the NIOUS images followed by measurement and correction of the shift was performed in these cases. Figure 4 shows appropriate correction of brain shift during excision of a cystic diffuse fibrillary astrocytoma in a 2-year-old boy.

NIOUS were more beneficial in tumors with cystic components (Figs. 1 and 3). Also, we found NIOUS of great help during detection of tumor residue and stepwise resection which could assist in achieving total excision. Residual tumors were located in the hidden rostral part of the cerebellar vermis in two cases and the lateral recess of the fourth ventricle in two other cases; thus, total excision was accomplished in most cases without much cerebellar retraction.

As regards the extent of surgical resection, total surgical excision was achieved in 29 cases (96.7 %) in NIOUS group versus 24 cases (80 %) in the conventional group. Regarding surgical morbidities, cerebellar mutism occurred in one case in the NIOUS group (3.3 %), as compared to six cases (20 %) of the conventional group.

In the NIOUS group, the cerebellar mutism case was of the mild and transient type. It involved the linguistic component only of the syndrome. It started 3 days postoperatively, and complete recovery occurred within 21 days.

On the other hand, cerebellar mutism cases among the conventional group were of the moderate and severe types. They started immediately postoperative, and one case showed incomplete recovery. Another case presented with mutism and

**Table 4** Distribution of age, operative time, and blood loss among the study groups

| Variables | Conventional group | | | NIOUS group | | | *p* value |
|---|---|---|---|---|---|---|---|
| | Min | Mean±SD | Max | Min | Mean SD | Max | |
| Age (years) | 1.00 | 4.96±2.55 | 12.00 | 1.50 | 5.58±2.73 | 14.00 | 0.37 |
| Operative time (min) | 110.00 | 140.66±18.60 | 180.00 | 120.00 | 150.00±18.28 | 185.00 | 0.055 |
| Blood loss (ml) | 50.00 | 71.00±15.44 | 110.00 | 40.00 | 67.50±17.00 | 100.00 | 0.40 |

*Max* maximum, *Min* minimum, *ml* milliliter, *SD* standard deviation

upper limb monoparesis that gradually improved over 6 months of follow-up and physiotherapy.

The lower incidence and severity of cerebellar mutism among the NIOUS cases may be attributed to applying less retraction force on the cerebellar nuclei, vermis, and superior cerebellar peduncles during the exploration and surgical manipulation in the rostral fourth ventricle and the lateral recesses, thus diminishing edema in these structures and preventing acute and permanent vascular insults. This may explain why the syndrome develops after a latent period of developing edema and why it is of the mild and transient type in the NIOUS group while it develops immediately postoperative and is of the severe type in the conventional group. It could be also attributed to possibility of violating the normal cerebellar tissue during resection in the brain–tumor interface, which could be avoided by obtaining updated intraoperative ultrasonographic images in a stepwise resection.

Although mean operative time was less in the conventional group than in the NIOUS group, there was no statistically significant difference between the two study groups ($p$ value=0.055). Thus, utilizing NIOUS during fourth ventricular tumor resection in children adds more safety to the surgery without significant prolongation of the duration of surgery. After a short learning curve, image quality of NIOUS was excellent and easily interpretable in all cases provided that the basic precautions for ultrasound examination are considered.

In our experience, we have observed that surgery of pediatric fourth ventricular tumors when assisted by NIOUS is more beneficial than using intraoperative ultrasound alone in these aspects:

1. Ultrasound image quality gets better if combined with neuro-navigation. This is because navigation aids in better identification of the tumor and surroundings hence minimizing tissue manipulation and subsequently, less tissue edema and less hyper-echoic artifacts.
2. It clearly detects hidden residual tumors after correcting the shift thus achieving safe total tumor excision.
3. It doesn't add much to the operative time.
4. It is not associated with a significant intraoperative blood loss.
5. It is an easily applicable and easily interpretable tool after a short learning curve.
6. It is cost-effective especially if compared to navigated intraoperative MRI.

Due to these potential benefits, we prefer the routine use of this technology during surgery of pediatric fourth ventricular tumors. However, there are some drawbacks for using NIOUS as it is not always easy to interpret ultrasonographic images whenever there is much edema or in infiltrative gliomas. These could be overcome after some experience in using ultrasound with the initial help of a radiologist. Also, combining and fusing the non-real-time neuro-navigator images with the 3D real-time ultrasound images needs cumulative experience especially in appreciating, calculating, updating, and correcting brain shifts. Studying a larger number of patients compared to navigated intraoperative MRI could be considered in our future research.

## Conclusions

The integration of navigated intraoperative ultrasonography in surgery of pediatric fourth ventricular tumors is a useful technology. It safely monitors maximum stepwise tumor excision. It is associated with less operative morbidity without significantly added operative time. It is also a real-time, cost-effective, easily applicable, and easily interpretable tool that could substitute the use of intraoperative MRI especially in pediatric neurosurgery.

**Disclosures** The authors have no personal, financial, institutional interest or industry affiliations in any of the drugs, materials, or devices described in this article.

## References


1. Akdemir H, Oktem IS, Menku A, Tucer B, Kamasak K, Tugcu B (2009) Neuronavigation by intraoperative ultrasound during intracranial cavernoma resection. Neurosurg Q 19:185–189
2. Aquilina K, Edwards P, Strong S (2006) Principles and practice of image-guided neurosurgery. In: Moore AJ, Newell DW (eds) Tumor neurosurgery principles and practice. Springer, London, p 132
3. Benveniste RJ, Germano I (2005) Correlation of factors predicting intraoperative brain shift with successful resection of malignant brain tumors using image guided techniques. Surg Neurol 63:542–549
4. Chen D, Wei X, Yin Q, Guan J, Pan W, Wang C, Liu Y (2009) The microscopic surgical treatment for tumor of posterior cranial fossa in children. Clin Oncol Cancer Res 6:95–99
5. El Beltagy MA, Aggag M, Kamal M (2010) Role of intraoperative ultrasound in resection of pediatric brain tumors. Childs Nerv Syst 26(9):1189–1193
6. Flitter MA, Buchheit WA, Murtagh F, Lapayowker MS (1975) Ultrasound determination of cerebrospinal fluid shunt patency. J Neurosurgery 42:728–730
7. Fu B, Zhao JZ, Yu LB (2008) The application of ultrasound in the management of cerebral arteriovenous malformation. Neurosci Bull 24(6):387–394
8. Hammoud MA, Ligon BL, ElSouki R, Shi WM, Schomer DR, Sawaya R (1996) Use of intraoperative ultrasound for localizing tumours and determining the extent of resection: a comparative study with magnetic resonance imaging. J Neurosurg 84:737–741
9. Huang X, Zhang J, Yang H, Yu T (2010) Use of intraoperative ultrasonography to monitor surgery for large acoustic neuromas: a pilot study. J Med Ultrasonics 37:15–19
10. Kanev PM, Foley CM, Miles D (1997) Ultrasound tailored functional hemispherectomy for surgical control of seizures in children. J Neurosurg 86:762–767

11. Koivukangas J, Louhisalmi Y, Alakuijala J, Oikarinen J (1993) Ultrasound-controlled neuronavigator-guided brain surgery. J Neurosurg 79:36–42
12. LeRoux PD, Berger MS, Ojemann GA, Wang K, Mack LA (1989) Correlation of intraoperative ultrasound tumour volumes and margins with preoperative computerized tomography scans. An intraoperative method to enhance tumour resection. J Neurosurg 71:691–698
13. Lindseth F, Ommedal S, Bang J, Unsgard G, Hernes TAN (2001) Image fusion of ultrasound and MRI as an aid for assessing anatomical shifts and improving overview and interpretation in ultrasound-guided neurosurgery. Int Congr Ser 1230:254–260
14. McGirt MJ, Attenello FJ, Datoo G, Gathinji M, Atiba ABS, Weingart JD, Carson B, Jallo GI (2008) Intraoperative ultrasonography as a guide to patient selection for duraplasty after suboccipital decompression in children with Chiari malformation type I. J Neurosurg Pediatrics 2:52–57
15. Nagle RC, Takeman MS, Shallat RF, Cohen RA (1986) Brain abscess aspiration in nursery with ultrasound guidance. J Neurosurg 65:557–559.12
16. Nimsky C, Ganslandt O, Hastreiter P, Fahlbusch R (2001) Intraoperative compensation for brain shift. Surg Neurol 56:357–365
17. Quencer RM, Montalvo BM (1986) Intraoperative cranial sonography. Neuroradiology 28:528–550
18. Ram Z, Shawker TH, Bradford MH, Doppman JL, Oldfield EH (1995) Intraoperative ultrasound-directed resection of pituitary tumors. J Neurosurg 83:225–230
19. Rasmussen A Jr, Lindseth F, Rygh OM, Berntsen EM, Selbekk T, Xu J, Nagelhus Hernes TA, Harg E, Haberg A, Unsgaard G (2007) Functional neuronavigation combined with intraoperative 3D ultrasound: initial experiences during surgical resections close to eloquent brain areas and future directions in automatic brain shift compensation of preoperative data. Acta Neurochir (Wien) 149:365–378
20. Rubin JM, Dohrmann GJ (1983) A cannula for use in ultrasonically guided biopsies of the brain. J Neurosurg 59:905–907
21. Solheim O, Selbekk T, Lindseth F, Unsgård G (2009) Navigated resection of giant intracranial meningiomas based on intraoperative 3D ultrasound. Acta Neurochir 151:1143–1151
22. Tanaka K, Ito K, Waga T (1964) The localization of brain tumors by ultrasonic techniques. A clinical review of 111 cases. J Neurosurgery 23:135–147
23. Wang Y, Wang Y, Dong Y, Wang Y (2006) The value of intraoperative ultrasonography in neurosurgery. J Med Ultrasonics 33:61–64
24. Wang Y, Wang Y, Wang Y, Taniguchi N, Chen XC (2007) Intraoperative real-time contrast-enhanced ultrasound angiography: a new adjunct in the surgical treatment of arteriovenous malformations. J Neurosurg 107:959–964
25. Whitehead WE, Jea A, Vachhrajani S, Kulkarni A, Drake JM (2007) Accurate placement of cerebrospinal fluid shunt ventricular catheters with real-time ultrasound guidance in older children without patent fontanelles. J Neurosurg (5 Suppl Pediatrics) 107:406–410
26. Yamasaio T, Moritake K, Takaya M, KagawaT NH, Akiyama Y, Kawahara M (1994) Intraoperative use of Doppler ultrasound and endoscopic monitoring in the stereotactic biopsy of malignant brain tumors. J Neurosurg 80:570–574
27. Zakrzewski K, Fiks T, Polis L, Liberski PP (2003) Posterior fossa tumours in children and adolescents. A clinicopathological study of 216 cases. Folia Neuropathol 41:251–252